

High-temperature electrical and thermal transport properties of fully filled skutterudites $\text{RFe}_4\text{Sb}_{12}$ ($\text{R} = \text{Ca, Sr, Ba, La, Ce, Pr, Nd, Eu, and Yb}$)

P. F. Qiu,^{1,2} J. Yang,¹ R. H. Liu,^{1,2} X. Shi,^{1,a)} X. Y. Huang,¹ G. J. Snyder,³ W. Zhang,⁴ and L. D. Chen¹

¹CAS Key Laboratory of Materials for Energy Conversion, Shanghai Institute of Ceramics, Chinese Academy of Sciences, 1295 Dingxi Road, Shanghai 200050, China

²Graduate University of Chinese Academy of Sciences, Beijing 100049, China

³Department of Materials Science, California Institute of Technology, 1200 East California Boulevard, Pasadena, California 91125, USA

⁴State Key Laboratory of High Performance Ceramics and Superfine microstructure, Shanghai Institute of Ceramics, Chinese Academy of Sciences, 1295 Dingxi Road, Shanghai 200050, China

(Received 15 November 2010; accepted 5 January 2011; published online 23 March 2011)

Fully filled skutterudites $\text{RFe}_4\text{Sb}_{12}$ ($\text{R} = \text{Ca, Sr, Ba, La, Ce, Pr, Nd, Eu, and Yb}$) have been prepared and the high-temperature electrical and thermal transport properties are investigated systematically. Lattice constants of $\text{RFe}_4\text{Sb}_{12}$ increase almost linearly with increasing the ionic radii of the fillers, while the lattice expansion in filled structure is weakly influenced by the filler valence charge states. Using simple charge counting, the hole concentration in $\text{RFe}_4\text{Sb}_{12}$ with divalent fillers ($\text{R} = \text{Ca, Sr, Ba, Eu, and Yb}$) is much higher than that in $\text{RFe}_4\text{Sb}_{12}$ with trivalent fillers ($\text{R} = \text{La, Ce, Pr, and Nd}$), resulting in relatively high electrical conductivity and low Seebeck coefficient. It is also found that $\text{RFe}_4\text{Sb}_{12}$ filled skutterudites having similar filler valence charge states exhibit comparable electrical conductivity and Seebeck coefficient, and the behavior of the temperature dependence, thereby leading to comparable power factor values in the temperature range from 300 to 800 K. All $\text{RFe}_4\text{Sb}_{12}$ samples possess low lattice thermal conductivity. The correlation between the lattice thermal resistivity W_L and ionic radii of the fillers is discussed and a good relationship of $W_L \sim (r_{\text{cage}} - r_{\text{ion}})^3$ is observed in lanthanide metal filled skutterudites. $\text{CeFe}_4\text{Sb}_{12}$, $\text{PrFe}_4\text{Sb}_{12}$, and $\text{NdFe}_4\text{Sb}_{12}$ show the highest thermoelectric figure of merit around 0.87 at 750 K among all the filled skutterudites studied in this work. © 2011 American Institute of Physics. [doi:10.1063/1.3553842]

I. INTRODUCTION

Filled skutterudites have been known as one of the best thermoelectric materials due to their excellent electrical performance and low lattice thermal conductivity.¹ The general structure formula of filled skutterudites is $\text{R}_y\text{M}_4\text{Sb}_{12}$, where R can be alkaline, alkaline-earth, lanthanide, or actinide metals, y is the filling fraction, and M is Fe, Ru, Os, Co, Rh, or Ir. Investigation on the thermoelectric properties in filled skutterudites has been initially started in 1990s.^{2–10} Earlier studies are mainly focused on p-type $\text{Fe}_x\text{Co}_{4-x}\text{Sb}_{12}$ -based compounds and the values of the dimensionless thermoelectric figure of merit (ZT) had been reported above unity.^{5,6,9,11,12} The progress in n-type filled skutterudites was rather slowly until partially filled skutterudites $\text{R}_y\text{Co}_4\text{Sb}_{12}$ with high filling fraction of the fillers were synthesized and reported with good thermoelectric performance at elevated temperature.^{13,14} After that, improving the thermoelectric figure of merit in n-type skutterudites gained keen interest in the next decade. Various n-type single element filled $\text{R}_y\text{Co}_4\text{Sb}_{12}$ skutterudites with high ZT values were reported,^{15,16} showing great potentials as thermoelectric power generator used at high temperatures. Moreover, recently, filling two or more types of fillers into the voids in skutterudite have been shown to be able to

further reduce lattice thermal conductivity and improve ZT to 1.4 in double-filled and 1.7 in multiple-filled n-type skutterudites.^{17–20} Although there are a series of recent study reported with very high ZT s in n-type partially filled skutterudites, only a few literatures focusing on high temperature thermoelectric properties in p-type skutterudites have been published in the past decade. Furthermore, the ZT values in p-type filled skutterudites are confirmed in experiment around 1.0, much lower than n-type materials.^{21–23} The stagnation of low ZT value in p-type skutterudites limits the further development of thermoelectric modules and devices, since both excellent n- and p-type materials are required for high efficiency thermoelectric technology. Therefore, searching for p-type skutterudites with comparable ZT values to n-type materials is urgent for real industry applications.

Recently, didymium-filled Fe-based p-type skutterudites were reported to exhibit high thermoelectric performance, indicating a continual interest in p-type skutterudites.²⁴ Because the formation of n-type double- and multiple-filled skutterudites has shown very effective to reduce lattice thermal conductivity and improve thermoelectric figure of merit, it might be also suitable for p-type skutterudites to achieve high ZT s. Therefore, systematic and deep understanding on the thermoelectric properties of single element filled skutterudites is necessary and urgent for the design and optimization in p-type double and multiple-filled skutterudites. Fully filled

^{a)}Electronic email: xshi@mail.sic.ac.cn.

skutterudites $\text{RFe}_4\text{Sb}_{12}$ is one of the most important p-type skutterudites. The first $\text{RFe}_4\text{Sb}_{12}$ compound was initially reported in 1980.²⁵ After that, various $\text{RFe}_4\text{Sb}_{12}$ ternary compounds with different filler elements were synthesized and reported with many interesting physical properties.^{3,4,6,8,10,26–38} However, the thermoelectric properties were only studied in a few $\text{RFe}_4\text{Sb}_{12}$ compounds experimentally.^{3,6,10,22,30,31} Furthermore, high temperature thermoelectric properties, which are crucial to the thermoelectric power generator, have been rarely reported in $\text{RFe}_4\text{Sb}_{12}$.^{6,10,31} Due to the lack of a broad systematic study, detailed understanding of the electrical and thermal transport properties in $\text{RFe}_4\text{Sb}_{12}$ system is still not available, which hinders the further optimization to achieve high ZT . Therefore, it is essential to gain a comprehensive understanding of electrical and thermal transport properties in single element filled $\text{RFe}_4\text{Sb}_{12}$ skutterudites.

In this paper, a series of $\text{RFe}_4\text{Sb}_{12}$ samples with various fillers ($R = \text{Ca}, \text{Sr}, \text{Ba}, \text{La}, \text{Ce}, \text{Pr}, \text{Nd}, \text{Eu},$ and Yb) were synthesized and the thermoelectric properties were measured in the temperature range from 300 to 800 K. Systematic evaluation and discussion related to the effects of these fillers on the crystal structure as well as thermoelectric properties were carried out.

II. EXPERIMENT

High purity elements were weighed out in the atomic ratio of $R : \text{Fe} : \text{Sb} = 1 : 4 : 12$, and then sealed in evacuated quartz ampoules which were coated with carbon. The sealed ampoules were heated slowly up to 1350 K for 10 hs, then quenched into a water bath and annealed at 773–973 K for 7 days. To form dense pellets, the obtained ingots were manually ground into fine powders ($<100 \mu\text{m}$) and then sintered by Spark Plasma Sintering (SPS) at 733–833 K for 10–15 mins. High-density ($>97\%$ of the theoretical density) were obtained for all samples. X-ray diffraction (XRD) analysis (Rigaku, Rint2000) and electron probe microanalysis (EPMA, Shimadzu 8705QH2) were used to examine the purity and chemical composition of the samples. Electrical conductivity (σ) and Seebeck coefficient (S) were measured using the ZEM-3 (ULVAC Co. Ltd.) apparatus under Helium atmosphere from 300 to 800 K. The thermal diffusivity and specific heat were measured in argon atmosphere using laser flash method (NETZSCH LFA 427) and Shimadzu DSC-50, respectively. The density of the samples was measured using Archimedes method. Total thermal conductivity (k) was calculated by multiplying the measured values of thermal diffusivity, specific heat, and density. Hall coefficients (R_H) at 300 K were measured in a Physical Property Measurement System (Quantum Design) by sweeping the magnetic field up to 3 T in both positive and negative directions.

III. RESULTS AND DISCUSSION

A. Phase structure, composition and lattice constant

1. XRD and EPMA results

Figure 1 shows the powder x-ray diffraction (XRD) patterns for all $\text{RFe}_4\text{Sb}_{12}$ samples. All peaks are identified as belonging to the $\text{LaFe}_4\text{P}_{12}$ structure. EPMA analyses show

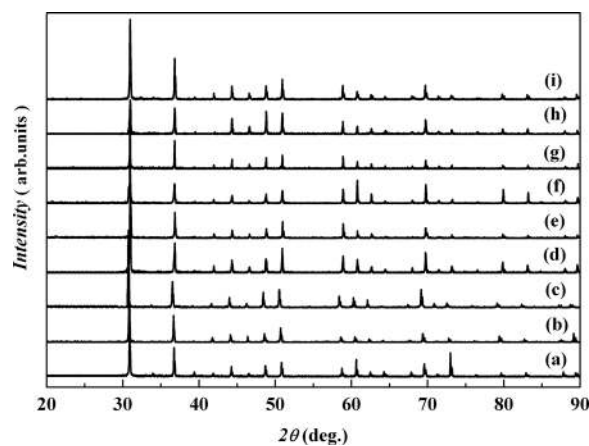


FIG. 1. XRD patterns for (a) $\text{CaFe}_4\text{Sb}_{12}$, (b) $\text{SrFe}_4\text{Sb}_{12}$, (c) $\text{BaFe}_4\text{Sb}_{12}$, (d) $\text{LaFe}_4\text{Sb}_{12}$, (e) $\text{CeFe}_4\text{Sb}_{12}$, (f) $\text{PrFe}_4\text{Sb}_{12}$, (g) $\text{NdFe}_4\text{Sb}_{12}$, (h) $\text{EuFe}_4\text{Sb}_{12}$, and (i) $\text{YbFe}_4\text{Sb}_{12}$.

that all samples contain trace amount of RSb_2 and Sb (less than 3%), which is not detected by XRD. Figure 2 shows the microstructure and element distribution of $\text{CeFe}_4\text{Sb}_{12}$. The energy dispersive spectroscopy (EDS) results indicate that all elements are distributed homogeneously in the matrix. The actual chemical compositions for all $\text{RFe}_4\text{Sb}_{12}$ samples determined by EPMA are shown in Table I. The final filling fraction of the fillers in all samples are less than 100%, being consistent with the published literatures.^{32,36,38} Although metastable $\text{Fe}_4\text{Sb}_{12}$ -based filled skutterudites with the entire sequence of lanthanides have been prepared using multilayer precursor approach,⁸ our attempt to synthesize lanthanides from Gd to Tm filled skutterudites using normal melting–quenching–annealing method was unsuccessful. The possible reason could be that the chemical bonds between the fillers and $[\text{Fe}_4\text{Sb}_{12}]$ framework are too weak to form thermodynamically stable materials under equilibrium conditions because of their very small ionic radius.²⁸

2. Lattice constant

Tang *et al.* reported that $\text{Fe}_x\text{Co}_{4-x}\text{Sb}_{12}$ is stable in the composition range of $x = 0 \sim 0.7$,³⁹ and the lattice constant (a) of this system obeys Vegard's law. The lattice constant of a " $\text{Fe}_4\text{Sb}_{12}$ " unit (a_0) could be extrapolated to be 9.125 Å under Vegard's law based on the reported data.^{1,39} Table I shows a of all $\text{RFe}_4\text{Sb}_{12}$ samples determined by an analytical extrapolation function of $(\cos^2\theta/\sin\theta + \cos^2\theta/\theta)/2$ using high-angle XRD data. Obviously, the increased a values in $\text{RFe}_4\text{Sb}_{12}$ are due to the extra lattice expansion by filling guest atoms into the voids in skutterudites. In order to identify the relationship, ionic radii of the fillers (r_{ion}) dependence of a for all $\text{RFe}_4\text{Sb}_{12}$ samples is shown in Fig. 3. Here, we use the r_{ion} values of the fillers with a coordination number of 12 for alkaline earths (Ca^{2+} , Sr^{2+} and Ba^{2+}) and lanthanides (La^{3+} , Ce^{3+} and Nd^{3+}).⁴⁰ There are no 12-coordinated r_{ion} values for Pr^{3+} , Eu^{2+} and Yb^{2+} , and the data used here are the extrapolated results using the relationship between the coordination number and effective r_{ion} in Ref. 40. Although the oxidation states could be +3 for both Eu and Yb, it had been reported and confirmed that the valence

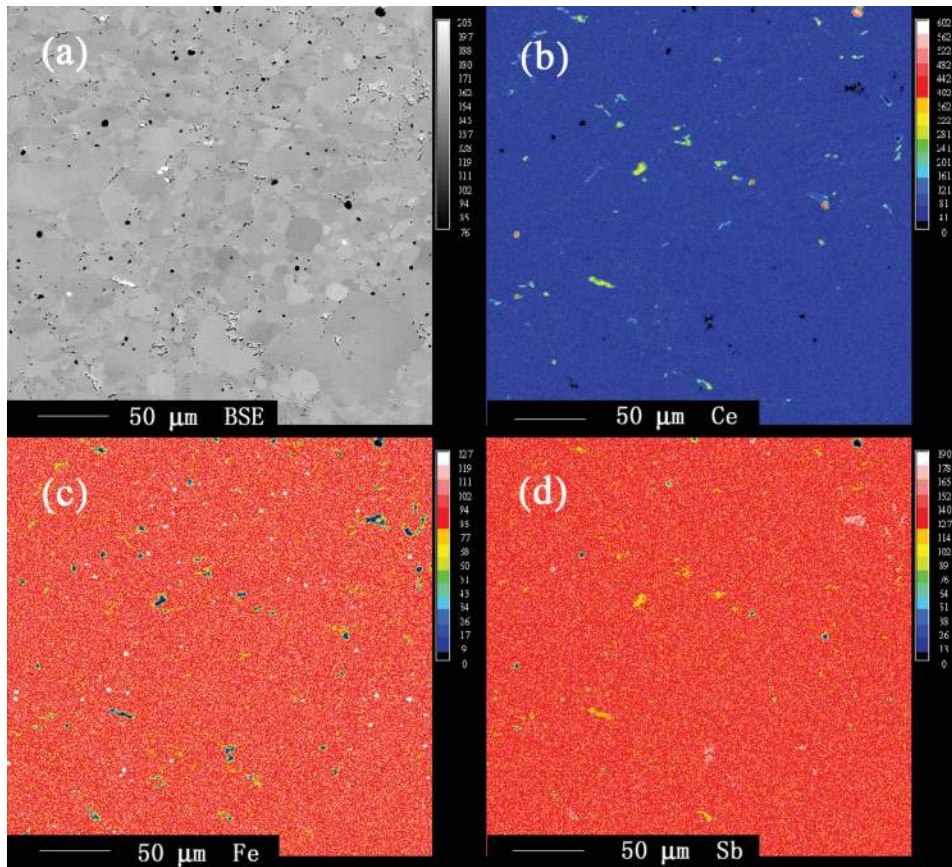


FIG. 2. (Color online) Microstructure and element distribution in sample $\text{CeFe}_4\text{Sb}_{12}$: (a) backscattered electron image (BSE); corresponding x-ray maps for Ce (b), Fe (c) and Sb (d) by energy dispersive spectroscopy (EDS).

charge states for Eu and Yb in skutterudites are close to $+2$ in filled skutterudites.^{28,31,41,42} These relatively large r_{ion} values of divalent Eu and Yb ion may enable Eu and Yb to form stable filled skutterudites.⁴³ For comparison, the reported a values for $\text{NaFe}_4\text{Sb}_{12}$, $\text{KFe}_4\text{Sb}_{12}$ and $\text{SmFe}_4\text{Sb}_{12}$ in literatures^{36,38} are also included in Fig. 3. A reasonably good correlation between expanded lattice constant and ion radius in $\text{RFe}_4\text{Sb}_{12}$ samples was observed. The lattice constant of the filled materials increases monotonously with increasing r_{ion} because larger fillers could expand lattice structure more significantly. The lattice constant of $\text{SmFe}_4\text{Sb}_{12}$ is around 9.1298 Å, close to the calculated value of “ $\text{Fe}_4\text{Sb}_{12}$.” If the ionic radii of the filler is less than Sm, the lattice constant of the filled structure might be compara-

ble or smaller than “ $\text{Fe}_4\text{Sb}_{12}$ ”, leading the filled structure thermodynamically unstable. This is further confirmed by our data that the synthesis of filled skutterudites with the fillers from Gd to Tm is unsuccessful. In addition, our data shows that the lattice constant in $\text{RFe}_4\text{Sb}_{12}$ is mainly determined by the ionic radius of the fillers, but not sensitive to the filler valence state (see Fig. 3).

Figure 3 also shows the relative increment of lattice constant ($\Delta a = (a - a_0)/a_0$) as a function of ionic radii of the fillers. Δa is less than 1% among all the fully filled skutterudites studied here. The slight deviation of lattice constant might scarcely affect the symmetry of the crystal structure, and thus exert little influence on the electrical transport properties. This provides a platform to discuss the effect of

TABLE I. Nominal and actual chemical composition, lattice constant, calculated chemical carrier concentration, and room temperature Hall carrier concentration, Seebeck coefficient, electrical conductivity, and lattice thermal conductivity for all $\text{RFe}_4\text{Sb}_{12}$ samples.

Nominal composition	EMPA composition	Lattice constant (Å)	Chemical carrier concentration ($10^{21} \times \text{cm}^{-3}$)	$1/R_{H\theta}$ ($10^{21} \times \text{cm}^{-3}$)	S ($\mu\text{V}/\text{K}$)	σ ($\times 10^5 \text{Sm}^{-1}$)	K_L ($\text{Wm}^{-1}\text{K}^{-1}$)
$\text{LaFe}_4\text{Sb}_{12}$	$\text{La}_{0.89}\text{Fe}_4\text{Sb}_{12.02}$	9.148	3.53	1.38	78.3	2.44	1.63
$\text{CeFe}_4\text{Sb}_{12}$	$\text{Ce}_{0.91}\text{Fe}_4\text{Sb}_{11.97}$	9.140	3.25	3.86	79.4	2.23	1.28
$\text{PrFe}_4\text{Sb}_{12}$	$\text{Pr}_{0.90}\text{Fe}_4\text{Sb}_{12.00}$	9.138	3.41	7.19	81.5	2.40	1.09
$\text{NdFe}_4\text{Sb}_{12}$	$\text{Nd}_{0.85}\text{Fe}_4\text{Sb}_{12.00}$	9.136	3.47	4.66	83.7	2.37	0.96
$\text{EuFe}_4\text{Sb}_{12}$	$\text{Eu}_{0.96}\text{Fe}_4\text{Sb}_{11.94}$	9.170	5.24	3.43	70.8	2.97	1.79
$\text{YbFe}_4\text{Sb}_{12}$	$\text{Yb}_{0.94}\text{Fe}_4\text{Sb}_{12.07}$	9.159	5.70	2.54	77.9	3.36	1.18
$\text{CaFe}_4\text{Sb}_{12}$	$\text{Ca}_{0.98}\text{Fe}_4\text{Sb}_{12.08}$	9.159	5.52	1.34	73.9	3.14	1.61
$\text{SrFe}_4\text{Sb}_{12}$	$\text{Sr}_{0.94}\text{Fe}_4\text{Sb}_{12.08}$	9.181	5.68	3.36	72.5	3.05	2.07
$\text{BaFe}_4\text{Sb}_{12}$	$\text{Ba}_{0.92}\text{Fe}_4\text{Sb}_{12.04}$	9.201	5.64	1.61	69.4	3.08	2.15

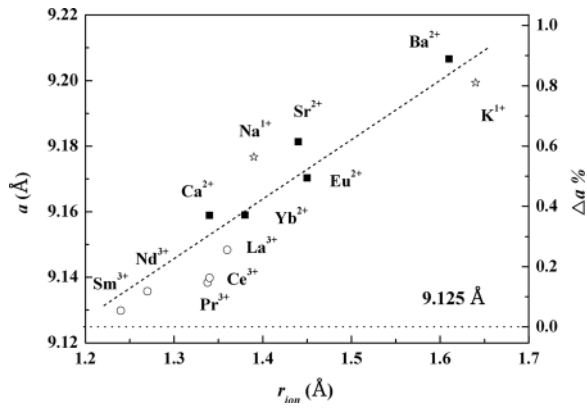


FIG. 3. Lattice constant and the relative increment of lattice constant Δa ($\Delta a = (a - a_0)/a_0$) as a function of ionic radii (12-coordinated) of the fillers in $\text{RFe}_4\text{Sb}_{12}$ ($\text{R} = \text{Ca}, \text{Sr}, \text{Ba}, \text{La}, \text{Ce}, \text{Pr}, \text{Nd}, \text{Eu}, \text{and Yb}$). Dashed line is guide to the eyes.

different fillers on the electrical transport properties in the following part.

B. Electrical transport properties

The temperature dependence of electrical conductivity (σ) and Seebeck coefficient (S) are shown in Fig. 4. Large σ values, with the magnitude of 10^5 S/m, are observed in all samples. In the whole temperature range investigated here, σ for all samples decreases monotonously with increasing temperature, which is typical heavily doped semiconducting behavior. All samples exhibit positive S values, showing that the majority of charge carriers are holes. Since Fe atom has one electron less than Co atom, a “ $\text{Fe}_4\text{Sb}_{12}$ ” unit is 4-electron

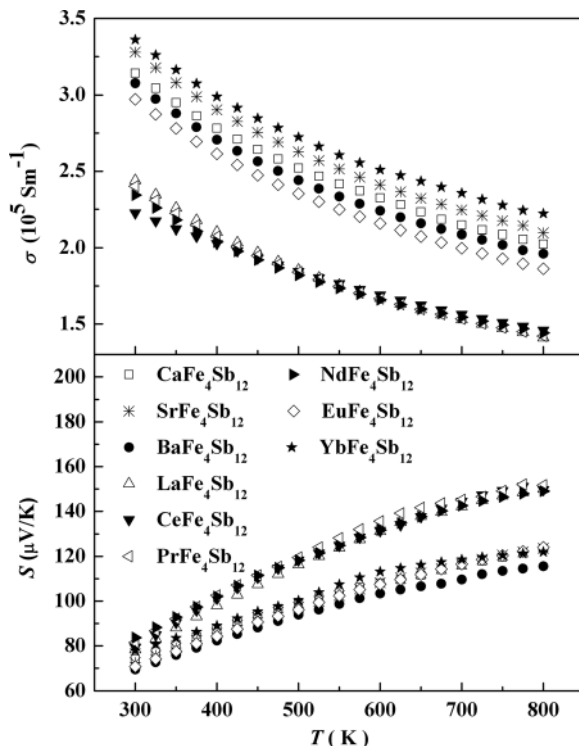


FIG. 4. Temperature dependence of electrical conductivity and Seebeck coefficient for all $\text{RFe}_4\text{Sb}_{12}$ samples ($\text{R} = \text{Ca}, \text{Sr}, \text{Ba}, \text{La}, \text{Ce}, \text{Pr}, \text{Nd}, \text{Eu}, \text{and Yb}$).

deficiency as compared with the binary semiconducting skutterudite $\text{Co}_4\text{Sb}_{12}$. Though the fillers in the voids donate their almost all valence electrons to the skutterudite framework, it is still insufficient to compensate the holes in fully filled skutterudites $\text{RFe}_4\text{Sb}_{12}$ because the oxidation states of the fillers are usually around +2 or +3. Hence, $\text{RFe}_4\text{Sb}_{12}$ system is expected to possess high hole density and positive S value. Table I shows the measured Hall carrier concentration p_H ($p_H = 1/R_H e$, where e is the elementary charge) at room temperature for all samples. Here, the Hall number is assumed to be 1 in the single carrier model. All samples are hole dominated with the carrier concentration on the order of 10^{21} cm^{-3} . The measured hole concentrations obviously deviate from the calculated values by simple charge counting based on the measured chemical compositions. Similar phenomenon has been also reported by Schnelle *et al.*³⁶ One possible reason might be related to the multiple bands near the Fermi level in $\text{RFe}_4\text{Sb}_{12}$ materials.³⁶ In this case, the understanding of the measured Hall coefficient is very complicated (there is no simple relationship between free carrier concentration p and R_H) and would require further systematic and detailed study. In addition, strong magnetic effects in $\text{RFe}_4\text{Sb}_{12}$ compounds may also contribute certainly to the anomalous Hall effect.³⁴ Therefore, in the following part, the calculated chemical carrier concentration (Table I) using simple electron counting are used for further discussion.

As shown in Fig. 4, $\text{RFe}_4\text{Sb}_{12}$ with divalent fillers ($\text{R} = \text{Ca}, \text{Sr}, \text{Ba}, \text{Eu}, \text{and Yb}$) exhibit higher σ and lower S than those in the trivalent lanthanide ($\text{R} = \text{La}, \text{Ce}, \text{Pr}, \text{and Nd}$) filled skutterudites. Because the divalent fillers in the voids donate one electron less than the trivalent fillers, the filled skutterudites ($\text{RFe}_4\text{Sb}_{12}$) with divalent fillers will possess higher hole densities and σ , and lower S values. The maximum S values at high temperature in $\text{RFe}_4\text{Sb}_{12}$ with divalent fillers are still higher than 100 $\mu\text{V/K}$. These high S values in $\text{Fe}_4\text{Sb}_{12}$ -based skutterudites might be related to the large effective mass of the holes due to the localized flat features of Fe-3d states near the Fermi level.^{4,44}

The electronic structure calculation by L. Nordström *et al.* suggested that $\text{CeFe}_4\text{Sb}_{12}$ is an intrinsic semiconductor where the 4f electron of Ce is completely donated into $[\text{Fe}_4\text{Sb}_{12}]$ framework.^{4,44} Simple electron counting also shows $\text{CeFe}_4\text{Sb}_{12}$ should be a semiconductor and the effective charge state of Ce is +4 if Ce-4f electron is completely transferred into $[\text{Fe}_4\text{Sb}_{12}]$ framework. However, our data indicate that $\text{CeFe}_4\text{Sb}_{12}$ exhibits metallic behavior with very high electrical conductivity, i.e., σ decreases with increasing temperature. This is consistent with other experimental results reported previously.^{3,21} Therefore, experimental data indicate that the effective charge state of Ce is not +4 in fully filled skutterudites, inconsistent with the theoretical calculations in Ref. 4. Hall measurement for Ce filled skutterudites by Chen *et al.* also demonstrated that the effective charge state of Ce is about +3,⁷ similar to the value in n-type filled skutterudites.⁴⁵ The difference between the experiment and theoretical calculations might be due to the difficulty of dealing with the strong-correlated 4f electron of Ce in the local density approximation. This problem may also exist in other p-type lanthanides filled skutterudites.

Interestingly, as shown in Fig. 4, $\text{RFe}_4\text{Sb}_{12}$ with trivalent fillers ($\text{R} = \text{La}, \text{Ce}, \text{Pr}, \text{and Nd}$) exhibit very similar σ and S values in the whole temperature range. In addition, $\text{RFe}_4\text{Sb}_{12}$ with divalent fillers ($\text{R} = \text{Ca}, \text{Sr}, \text{Ba}, \text{Eu}, \text{and Yb}$) also show similar σ and S values although the deviations are large. In general, σ and S are predominantly determined by the hole concentration and band structure near the Fermi level. Our data likely indicate that the fillers, particularly lanthanides $\text{La}, \text{Ce}, \text{Pr}, \text{and Nd}$, show similar effect on the band edge near the Fermi level. Then, the similar electronic structure of these several lanthanides filled $\text{RFe}_4\text{Sb}_{12}$ would lead to small difference in the observed σ and S . The band structures of $\text{CeFe}_4\text{Sb}_{12}$ and $\text{LaFe}_4\text{Sb}_{12}$ were calculated by K. Nouneh *et al.*⁴⁴ It was shown that the primary valence band of both $\text{CeFe}_4\text{Sb}_{12}$ and $\text{LaFe}_4\text{Sb}_{12}$ are the hybridized Sb-5p orbital and Fe-3d orbital. The $4f$ and $5d$ orbitals of Ce only contribute to the conduction band. Optical reflectivity measurement and electronic structure calculation in $\text{RFe}_4\text{Sb}_{12}$ ($\text{R} = \text{Ca}, \text{Ba}, \text{and Yb}$) Ref. 35 also suggested that they possess similar valence band structure. All these results seem to be consistent with our arguments mentioned above. Systematic study on the band structures in $\text{RFe}_4\text{Sb}_{12}$ is needed to get a fully comprehensive understanding of the observed experimental results.

Figure 5 shows the power factor ($PF = S^2\sigma$) as a function of temperature for all samples. Due to the comparable electrical transport properties, $\text{RFe}_4\text{Sb}_{12}$ with the trivalent fillers possess similar PF values in the whole temperature range. Except $\text{YbFe}_4\text{Sb}_{12}$, PF values of $\text{RFe}_4\text{Sb}_{12}$ with divalent fillers are lower than those with trivalent fillers because of their smaller S values. The maximum value around $34 \mu\text{W}/\text{cmK}^2$ is obtained in $\text{CeFe}_4\text{Sb}_{12}$, $\text{PrFe}_4\text{Sb}_{12}$, and $\text{YbFe}_4\text{Sb}_{12}$ at 750 K.

C. Thermal transport properties

1. Thermal conductivity and lattice thermal conductivity

Figure 6(a) shows the temperature dependence of thermal conductivity (κ) for all $\text{RFe}_4\text{Sb}_{12}$ samples. Here, the measured specific heat (C_p) of $\text{CeFe}_4\text{Sb}_{12}$ is used for calcu-

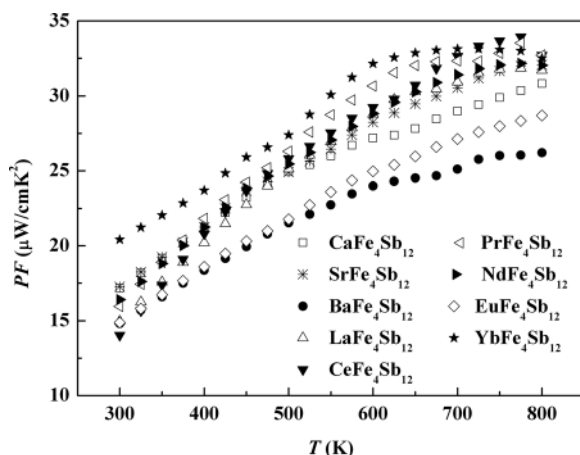


FIG. 5. Temperature dependence of power factor for all $\text{RFe}_4\text{Sb}_{12}$ samples ($\text{R} = \text{Ca}, \text{Sr}, \text{Ba}, \text{La}, \text{Ce}, \text{Pr}, \text{Nd}, \text{Eu}, \text{and Yb}$).

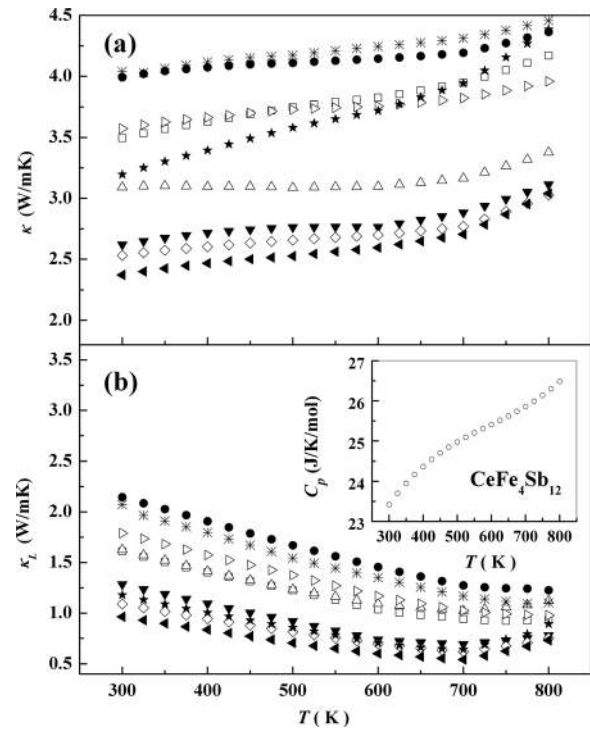


FIG. 6. Temperature dependence of (a) thermal conductivity and (b) lattice thermal conductivity for all $\text{RFe}_4\text{Sb}_{12}$ samples ($\text{R} = \text{Ca}: \square, \text{Sr}: *, \text{Ba}: \bullet, \text{La}: \square, \text{Ce}: \blacktriangledown, \text{Pr}: \triangle, \text{Nd}: \blacktriangleright, \text{Eu}: \square, \text{and Yb}: \square$). The inset shows the specific heat for sample $\text{CeFe}_4\text{Sb}_{12}$ above room temperature.

lating κ for all samples because of their almost identical C_p values above room temperature. As shown in the insert of Fig. 6, C_p of sample $\text{CeFe}_4\text{Sb}_{12}$ increases with increasing temperature. It reaches 26.2 J/g/mol at 800 K, about 15% higher than that at 300 K. In the whole temperature range investigated here, all the κ values increase with increasing temperature. The total κ is a sum of two contributions: lattice thermal conductivity (κ_L) and carrier thermal conductivity (κ_c). According to the Wiedemann–Franz law, κ_c can be estimated by $\kappa_c = L_0 T \sigma$ under single carrier approximation (where the Lorenz number L_0 has an empirical value of $2.0 \times 10^{-8} \text{ V}^2 \text{K}^{-2}$ for skutterudite compounds^{9,11}). Consequently, κ_L can be obtained by subtracting the carrier part from the measured κ . This assessment of κ_L is only an approximation due to the lack of precise L_0 value and its uncertain temperature dependence for this degenerate semi-conducting system. However, this method can provide a mechanism for comparing the existing κ_L values for all $\text{RFe}_4\text{Sb}_{12}$ samples. Figure 6(b) shows the temperature dependence of κ_L for all samples. The lowest κ_L value in $\text{RFe}_4\text{Sb}_{12}$ is around 1.0 W/mK at room temperature and 0.6 W/mK at 700 K, comparable to or lower than $\alpha\text{-SiO}_2$. One possible mechanism for such low κ_L in filled skutterudites is the “rattling” effect of the loosely bonded guest fillers in the skutterudite voids. These guest fillers interact strongly with the low-frequency acoustic phonons, leading to partial energy of the phonons being trapped in the excited rattling state. This part of phonons would later decay into phonons incoherent with those of the absorbed phonons, and thus contribute to the lowered κ_L .^{17,46,47}

As shown in Fig. 6(b), below 700 K, κ_L for all samples decreases with increasing temperature, indicating that phonon transport is hindered by the dynamical process of Umklapp scattering. κ_L for $\text{RFe}_4\text{Sb}_{12}$ with trivalent fillers ($\text{R} = \text{La}, \text{Ce}, \text{Pr}, \text{and Nd}$) reach the minimum values around 700 K, then slightly increase with increasing temperature. This is due to the additional heat carried by the electron-hole pair generated from intrinsic excitation at high temperatures (bipolar diffusion). In fact, bipolar diffusion is an inherent feature in p-type filled skutterudites because of its narrow bandgap. In order to improve ZT in p-type filled skutterudites, one would like to reduce the bipolar diffusion effect to make κ_L continually decreasing at high temperature. One possible method is to increase the hole concentration to shift the turning point of κ_L to higher temperature. As shown in Fig. 6(b), κ_L for $\text{RFe}_4\text{Sb}_{12}$ ($\text{R} = \text{Ca}, \text{Sr}, \text{Ba}, \text{and Eu}$) decreases monotonously in the entire temperature range due to their larger hole concentration. However, the enhanced carrier concentration definitely increases κ_c and deteriorates S simultaneously, which could lower the overall thermoelectric performance. Therefore, other approaches (e.g., enlarging bandgap) are recommended to reduce the effect of bipolar diffusion to achieve higher ZT values.

2. Correlation between lattice thermal conductivity and ionic radii of the trivalent fillers

Since all the samples have similar filling fraction (y) (as shown in Table I), it is possible to evaluate the effect of different fillers on the κ_L reduction systematically. In filled skutterudites, based on the assumption that the effect of the additional κ_L reduction by the fillers is a localized behavior,⁴⁸ total lattice thermal resistivity W_L ($=1/\kappa_L$) could be written as $W_L = W_{\text{matrix}} + W_{PD} + W_R$, where W_{matrix} is the thermal resistivity of the $[\text{Fe}_4\text{Sb}_{12}]$ framework, W_{PD} is the thermal resistivity contributed by point defect, and W_R is the thermal resistivity contributed by resonant scattering due to the local rattling of guest fillers, respectively. In principle, W_{PD} includes the effect of structure strain (W_S) and mass fluctuation (W_M) between the void and filler.⁴⁹ Here, the data are compared among these nearly fully filled skutterudites in an attempt to get a systematic understanding on the κ_L reduction. The additional effect of strain fluctuation on the κ_L reduction might be neglected because of the small deviation (less than 1%) of lattice constant among all the fully filled skutterudites mentioned above. Since the atomic weight (M) for the rare earth atoms La, Ce, Pr, Nd, and Eu are very close, W_M for $\text{RFe}_4\text{Sb}_{12}$ ($\text{R} = \text{La}, \text{Ce}, \text{Pr}, \text{Nd}$ and Eu) are also similar to each other. Therefore, in these fully filled skutterudites, phonon resonant scattering might be the only mechanism to make κ_L values in $\text{RFe}_4\text{Sb}_{12}$ ($\text{R} = \text{La}, \text{Ce}, \text{Pr}, \text{Nd}, \text{and Eu}$) different with each other. As we know, the chemical bonds between the filler and skutterudite framework are mainly ionic,⁴⁵ thus the bond energy is approximately in proportion to $1/\Delta r$.⁵⁰ Thus, for a resonant scattering, W_R is almost in proportion to $1/(\Delta r)^3$, where Δr is the distance between the positive charge of filler ion and the negative charge of its nearest Sb anion, and thus equal to $(r_{\text{cage}} - r_{\text{ion}})$. Here, r_{cage} is the Sb-icosahedron void radius in $\text{RFe}_4\text{Sb}_{12}$ and an average value of 1.94 Å is used in this paper.¹ Figure 7

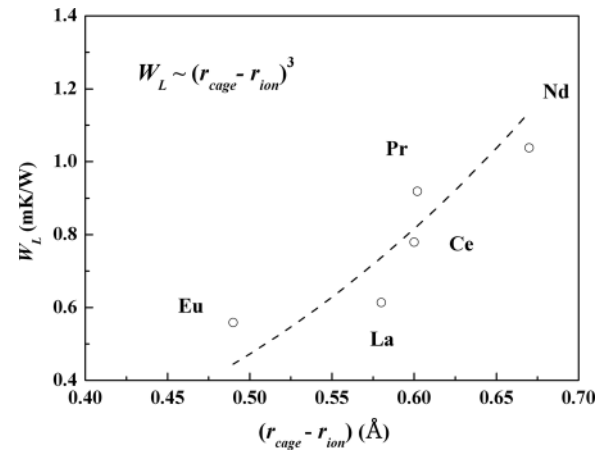


FIG. 7. Room temperature W_L as a function of $(r_{\text{cage}} - r_{\text{ion}})$ for $\text{RFe}_4\text{Sb}_{12}$ ($\text{R} = \text{La}, \text{Ce}, \text{Pr}, \text{Nd}, \text{and Eu}$). Dashed line represents the relationship of $W_L \sim (r_{\text{cage}} - r_{\text{ion}})^3$ (Ref. 3).

shows W_L at 300 K as a function of $(r_{\text{cage}} - r_{\text{ion}})$ for $\text{RFe}_4\text{Sb}_{12}$ ($\text{R} = \text{La}, \text{Ce}, \text{Pr}, \text{Nd}, \text{and Eu}$) samples. A good relationship of $W_L \sim (r_{\text{cage}} - r_{\text{ion}})^3$ (Ref. 3) is observed in these fully filled skutterudites. Larger $(r_{\text{cage}} - r_{\text{ion}})$ value indicates that the fillers are more loosely bonded with $[\text{Fe}_4\text{Sb}_{12}]$ framework. The stronger “rattling” effect can greatly scatter heat carrying phonons, thereby enhancing W_L . For example, $\text{NdFe}_4\text{Sb}_{12}$ has the largest $(r_{\text{cage}} - r_{\text{ion}})$ value investigated here. At the same time, it has the highest W_L among all the samples.

D. Dimensionless thermoelectric figure of merit ZT

Figure 8 shows the dimensionless figure of merit (ZT) calculated based on the measured σ , S and κ . As a result of larger S and lower κ , $\text{RFe}_4\text{Sb}_{12}$ with trivalent fillers ($\text{R} = \text{La}, \text{Ce}, \text{Pr}, \text{and Nd}$) exhibit higher ZT values than those with divalent fillers ($\text{R} = \text{Ca}, \text{Sr}, \text{Ba}, \text{Eu}, \text{and Yb}$). $\text{CeFe}_4\text{Sb}_{12}$, $\text{PrFe}_4\text{Sb}_{12}$, and $\text{NdFe}_4\text{Sb}_{12}$ exhibit the maximum ZT value, about 0.87 at 750 K.

Figure 9 plots the ZT values as a function of the filler ionic radii for all $\text{RFe}_4\text{Sb}_{12}$ samples at 300 K and 800 K,

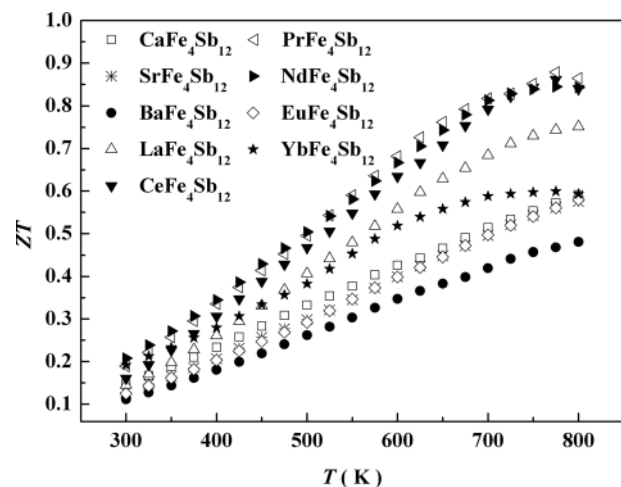


FIG. 8. Temperature dependence of ZT for all $\text{RFe}_4\text{Sb}_{12}$ compounds ($\text{R} = \text{Ca}, \text{Sr}, \text{Ba}, \text{La}, \text{Ce}, \text{Pr}, \text{Nd}, \text{Eu}, \text{and Yb}$).

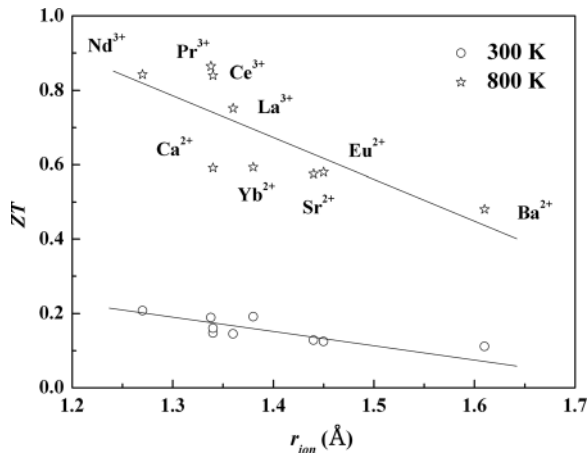


FIG. 9. ZT as a function of r_{ion} for all RFe_4Sb_{12} compounds ($R = Ca, Sr, Ba, La, Ce, Pr, Nd, Eu,$ and Yb) at 300 K and 800 K. The dashed lines are guide to the eyes.

respectively. A general trend, i.e., small r_{ion} corresponds with higher ZT , can be observed. This result might provide a straightforward image to design or search novel compositions to realize high ZT values in filled skutterudites.

IV. CONCLUSION

In summary, a systematic study has been carried out on RFe_4Sb_{12} skutterudites filled with alkaline earth (Ca, Sr, and Ba) and lanthanides metals (La, Ce, Pr, Nd, Eu, and Yb). For all RFe_4Sb_{12} samples, lattice constant a increases with increasing r_{ion} . σ , S and κ for all samples are measured in the temperature range from 300 to 800 K. Since divalent fillers donate two electrons and trivalent fillers donate three electrons to compensate the holes in $[Fe_4Sb_{12}]$ framework, RFe_4Sb_{12} ($R = Ca, Sr, Ba, Eu,$ and Yb) show large σ and small S values as compared with those in RFe_4Sb_{12} with trivalent fillers ($R = La, Ce, Pr,$ and Nd). RFe_4Sb_{12} skutterudites with similar filler valence charge state exhibit very close σ and S values. The maximum power factor value around $34 \mu W/cmK^2$ is obtained for $CeFe_4Sb_{12}$, $PrFe_4Sb_{12}$, and $YbFe_4Sb_{12}$ at 750 K. All samples possess low κ_L due to the “rattling” effect of the fillers, which could scatter low-frequency heat carrying phonons. For RFe_4Sb_{12} with trivalent fillers ($R = La, Ce, Pr,$ and Nd), the slight increase of κ_L above 700 K can be explained by the bipolar diffusion caused by the intrinsic excitation, which is not observed in RFe_4Sb_{12} with divalent fillers ($R = Ca, Sr, Ba, Eu,$ and Yb). The effect of the ionic radii of the fillers on thermal transport properties is discussed. It is found that κ_L decreases with increasing r_{ion} for samples RFe_4Sb_{12} ($R = La, Ce, Pr, Nd,$ and Eu). A maximum ZT value of 0.87 is obtained in $CeFe_4Sb_{12}$, $PrFe_4Sb_{12}$ and $NdFe_4Sb_{12}$. In addition, an empirical trend between the ionic radii of the fillers and the thermoelectric figure of merit is proposed. Fillers with small r_{ion} correspond to higher ZT values. This provides a straightforward trend to choose fillers to realize high ZT values in skutterudites. Our work offers a systematic understanding on the thermoelectric transport properties in RFe_4Sb_{12} and presents

much useful information for further design and optimization in Fe_4Sb_{12} -based skutterudites.

ACKNOWLEDGMENTS

This work was partly supported by National Natural Science Foundation of China (Nos. 50802109, 50820145203, 50825205), and the Visiting Professor and Knowledge Innovation Programs of the Chinese Academy of Sciences (Contract No. KJCX2-YW-H20).

- ¹L. D. Chen, *Proceedings of the 21st International Conference of Thermoelectrics* (IEEE, New York, 2002), p. 42.
- ²B. C. Sales, D. Mandrus, and R. K. Williams, *Science* **272**, 1325 (1996).
- ³D. T. Morelli and G. P. Meisner, *J. Appl. Phys.* **77**, 3777 (1995).
- ⁴L. Nordström, D. J. Singh, *Phys. Rev. B* **53**, 1103 (1996).
- ⁵J.-P. Fleurial, A. Borshechsky, and T. Caillat, *Proceedings of the 15th International Conference of Thermoelectrics* (IEEE, New York, 1996), p. 91.
- ⁶J.-P. Fleurial, T. Caillat, and A. Borshechsky, *Proceedings of the 16th International Conference of Thermoelectrics* (IEEE, New York, 1997), p. 1.
- ⁷B. X. Chen, J. H. Xu, C. Uher, D. T. Morelli, G. P. Meisner, J. -P. Fleurial, T. Caillat, and A. Borshechsky, *Phys. Rev. B* **55**, 1476 (1997).
- ⁸M. D. Hornbostel, E. J. Hyer, J. H. Edvalson, and D. C. Johnson, *Inorg. Chem.* **36**, 4270 (1997).
- ⁹B. C. Sales, D. Mandrus, B. C. Chakoumakos, V. Keppens, and J. R. Thompson, *Phys. Rev. B* **56**, 15081 (1997).
- ¹⁰D. M. Rowe, V. L. Kuznetsov, and L. A. Kuznetsova, *Proceedings of the 17th International Conference of Thermoelectrics* (IEEE, New York, 1998), p. 323.
- ¹¹X. F. Tang, L. D. Chen, T. Goto, and T. Hirai, *J. Mater. Res.* **16**, 837 (2001).
- ¹²X. F. Tang, L. D. Chen, T. Goto, T. Hirai, and R. Z. Yuan, *J. Mater. Sci.* **36**, 5435 (2001).
- ¹³G. S. Nolas, H. Takizawa, T. Endo, H. Sellinschegg, and D. C. Johnson, *Appl. Phys. Lett.* **77**, 52 (2000).
- ¹⁴L. D. Chen, T. Kawahara, X. F. Tang, T. Goto, T. Hirai, J. S. Dyck, W. Chen, and C. Uher, *J. Appl. Phys.* **90**, 1864 (2001).
- ¹⁵V. L. Kuznetsov, L. A. Kuznetsova, and D. M. Rowe, *J. Phys. Condens. Matter.* **15**, 5035 (2003) (and references therein).
- ¹⁶Y. Z. Pei, L. D. Chen, W. Zhang, X. Shi, S. Q. Bai, X. Y. Zhao, Z. G. Mei, and X. Y. Li, *Appl. Phys. Lett.* **89**, 221107 (2006) (and references therein).
- ¹⁷J. Yang, W. Zhang, S. Q. Bai, Z. Mei, and L. D. Chen, *Appl. Phys. Lett.* **90**, 192111 (2007).
- ¹⁸S. Q. Bai, Y. Z. Pei, L. D. Chen, W. Q. Zhang, X. Y. Zhao, and J. Yang, *Acta Mater.* **57**, 3135 (2009).
- ¹⁹X. Shi, H. Kong, C-P. Li, C. Uher, J. Yang, J. R. Salvador, H. Wang, L. D. Chen, and W. Zhang, *Appl. Phys. Lett.* **92**, 182101 (2008).
- ²⁰X. Shi, J. Yang, J. R. Salvador, M. Chi, J. Y. Cho, H. Wang, S. Bai, J. Yang, W. Zhang, and L. Chen, Multiple-filled skutterudites: High thermoelectric figure of merit through separately optimizing electrical and thermal transports, submitted.
- ²¹D. Bérardan, E. Alleno, C. Godart, M. Puyet, B. Lenoir, R. Lackner, E. Bauer, L. Girard, and D. Ravot, *J. Appl. Phys.* **98**, 033710 (2005).
- ²²X. F. Tang, H. Li, Q. J. Zhang, M. Niino, and T. Goto, *J. Appl. Phys.* **100**, 123702 (2006).
- ²³P. N. Alboni, X. Ji, J. He, N. Gothard, and T. M. Tritt, *J. Appl. Phys.* **103**, 113707 (2008).
- ²⁴G. Rogl, A. Grytsiv, E. Bauer, P. Rogl, and M. Zehetbauer, *Intermetallics* **06**, 005 (2009).
- ²⁵D. J. Braun and W. Jeitschko, *J. Less-Common Met.* **72**, 147 (1980).
- ²⁶C. B. H. Evers, W. Jeitschko, L. Boonk, D. J. Braun, Th. Ebel, and U. D. Scholz, *J. Alloys. Comp.* **184**, 224 (1995).
- ²⁷V. Keppens, D. Mandrus, B. C. Sales, B. C. Chakoumakos, P. Dai, R. Coldea, M. B. Maple, D. A. Gajewski, E. J. Freeman, and S. Bennington, *Nature* **395**, 876 (1998).
- ²⁸N. R. Dilley, E. J. Freeman, E. D. Bauer, and M. B. Maple, *Phys. Rev. B* **58**, 6287 (1998).
- ²⁹J. W. Kaiser and W. Jeitschko, *J. Alloys. Comp.* **291**, 66 (1999).
- ³⁰N. R. Dilley, E. D. Bauer, M. B. Maple, S. Dordevic, D. N. Basov, F. Freiberger, T. W. Darling, A. Migliori, B. C. Chakoumakos, and B. C. Sales, *Phys. Rev. B* **61**, 4608 (2000).

- ³¹V. L. Kuznetsov and D. M. Rowe, *J. Phys. Condens. Matter.* **12**, 7915 (2000).
- ³²E. Bauer, St. Berger, Ch. Paul, M. Della Mea, G. Hilscher, H. Michor, M. Reissner, W. Steiner, A. Grytsiv, P. Rogl, and E. W. Scheidt, *Phys. Rev. B* **66**, 214421 (2002).
- ³³A. Leithe-Jasper, W. Schnelle, H. Rosner, M. Baenitz, A. Rabis, A. A. Gippius, E. N. Morozova, H. Bormann, U. Burkhardt, R. Ramlau, U. Schwarz, J. A. Mydosh, and Y. Grin, *Phys. Rev. B* **70**, 214418 (2004).
- ³⁴B. C. Sales, R. Jin, D. Mandrus, and P. Khalifah, *Phys. Rev. B* **73**, 224435 (2006).
- ³⁵J. Sichelschmidt, V. Voevodin, H. J. Im, S. Kimura, H. Rosner, A. Leithe-jasper, W. Schnelle, U. Burkhardt, J. A. Mydosh, Yu. Grin, and F. Steglich, *Phys. Rev. Lett.* **96**, 037406 (2006).
- ³⁶W. Schnelle, A. Leithe-Jasper, H. Rosner, R. Cardoso-Gil, R. Gumeniuk, D. Trots, J. A. Mydosh, and Y. Grin, *Phys. Rev. B* **77**, 094421 (2008).
- ³⁷M. M. Koza, M. R. Johnson, R. Viennois, H. Mutka, L. Girard, and D. Ravot, *Nat. Mater.* **7**, 805 (2008).
- ³⁸M. Ueda, Y. Kawahito, K. Tanaka, D. Kikuchi, H. Aoki, H. Sugawara, K. Kuwahara, Y. Aoki, and H. Sato, *Physica B* **403**, 881 (2008).
- ³⁹X. F. Tang, L. D. Chen, T. Goto, and T. Hirai, *Jpn. Inst. Metals.* **63**, 1412 (1999).
- ⁴⁰R. D. Shannon, *Acta Cryst.* **A32**, 751 (1976).
- ⁴¹A. Grytsiv, P. Rogl, St. Berger, Ch. Paul, E. Bauer, B. Ni, M. M. Abd-Elmeguid, A. Saccone, R. Ferro, and D. Kaczorowski, *Phys. Rev. B* **66**, 094411 (2002).
- ⁴²J. Yang, L. Xi, W. Zhang, L. D. Chen, and J. Yang, *J. Electron Mater.* **38**, 1397 (2009).
- ⁴³Z. G. Mei, J. Yang, Y. Z. Pei, W. Zhang, L. D. Chen, and J. Yang, *Phys. Rev. B* **77**, 045202 (2008).
- ⁴⁴K. Nouneh, Ali. H. Reshak, S. Auluck, I. V. Kityk, R. Viennois, S. Benet, and S. Charar *J. Alloys. Compd.* **437**, 39 (2007).
- ⁴⁵X. Shi, W. Zhang, L. D. Chen, J. Yang, and C. Uher, *Phys. Rev. B* **75**, 235208 (2007).
- ⁴⁶G. J. Long, R. P. Hermann, F. Grandjean, E. E. Alp, W. Sturhahn, C. E. Johnson, D. E. Brown, O. Leupold, and R. Rüffer, *Phys. Rev. B* **71**, 140302 (2005).
- ⁴⁷E. R. Grannan, M. Randeria, and J. P. Sethna, *Phys. Rev. B* **41**, 7799 (1990).
- ⁴⁸J. L. Cohn, G. S. Nolas, V. Fessatidis, T. H. Metcalf, and G. A. Slack, *Phys. Rev. Lett.* **82**, 779 (1999).
- ⁴⁹G. A. Slack, *Phys. Rev.* **105**, 829 (1957).
- ⁵⁰C. Kittel, in *Introduction to Solid State Physics*, 8th ed. (John Wiley and Sons, New York, 2005), p. 63.